

Derivation of Interatomic Potentials for Gallophosphates from the GaPO₄–Quartz Structure: Transferability Study to Gallosilicates and Zeotype Gallophosphates

Stéphanie Girard,[†] Julian D. Gale,[‡] Caroline Mellot-Draznieks,^{*,†} and Gérard Férey^{*,†}

Institut Lavoisier, Université de Versailles Saint Quentin, 45 avenue des Etats-Unis, F-78035 Versailles Cedex, France, and Department of Chemistry, Imperial College of Science, Technology and Medicine, South Kensington SW7 2AY, U.K.

Received November 27, 2000. Revised Manuscript Received February 20, 2001

A new force field for gallium in gallophosphate microporous solids has been derived, using a formal charge shell model chosen for its compatibility with existing potentials for zeolites and their aluminophosphate analogues. Potentials for gallium were obtained empirically by fitting against the dense structure of GaPO₄–quartz and its physical properties. The calculations on various model gallosilicate structures, including gallium in various coordinations (IV, VI), demonstrate the transferability of the new force field to another class of compounds. Finally, our potential reproduces model gallophosphate structures having zeotype architectures with reasonable accuracy, ensuring its validity for further studies of open-framework gallophosphates.

Introduction

During the past decade, the chemical diversity of open-framework inorganic structures has been relentlessly extending. Following the development of synthetic silicate/aluminosilicate zeolites and the discovery of their aluminophosphate analogues, new families of compounds have been explored on the basis of metal substitution of the framework atoms.^{1,2} In this context, since the first gallophosphate synthesis by Parise,³ the exploration of gallium phosphates (GaPOs) has given rise to a wide diversity of structures, including those of zeotypes⁴ and a large variety of three-dimensional open-framework materials, besides numerous layered and chain solids. For example, a whole series of new oxy-fluorinated three-dimensional structures have been discovered, starting with the extra-large-pore cloverite framework,⁵ a number of structures of the ULM-*n* and MIL-*n* families,⁶ and the Mu-*n* series of compounds.⁷

Atomistic simulations have now become a major tool for understanding the structures and properties of

materials⁸ through the development of interatomic potentials aimed at reproducing geometries accurately, such as cell parameters, bond lengths, and bond angles. The validity of the force field has to be addressed through the simulations of a well-characterized reference structure and its physical properties. The transferability of the force field may then be efficiently tested through the simulations of polymorphs of the reference structure.

Typically, silica polymorphs and aluminophosphates have benefited from the development of specific empirical or ab initio derived force fields.^{9–13} Sanders¹⁰ and Henson et al.^{11–13} derived force fields for silica and AlPOs using an empirical fit to the crystal structures and physical properties of α -quartz (SiO₂) and berlinite (AlPO₄), respectively. Their formal charge shell model force fields have been shown to reproduce a whole series of experimentally determined structures of silicates¹¹ and aluminophosphates¹³ with reasonable accuracy and to yield estimates of their relative framework stabilities that are consistent with thermodynamic data. The phase stishovite, which contains octahedrally coordinated atoms, is excluded from this, since the form of the force field precludes it from correctly treating this material. More recently, lattice energy minimizations using the force field of Gale and Henson¹² have allowed

[†] Université de Versailles Saint Quentin.

[‡] Imperial College of Science, Technology and Medicine.

(1) Cheetham, A. K.; Férey, G.; Loiseau, T. *Angew. Chem., Int. Ed.* **1999**, *38*, 3268.

(2) Hartman, M.; Kevan, L. *Chem. Rev.* **1999**, *99*, 635.

(3) Parise, J. B. *Inorg. Chem.* **1985**, *24*, 4312. Parise, J. B. *J. Chem. Soc., Chem. Commun.* **1985**, 606. Parise, J. B. *Acta Crystallogr.* **1986**, *C42*, 670.

(4) Meier, W. M.; Olson, D. H.; Baerlocher, C. *Atlas of Zeolite Structure Types*; Elsevier: London, 1996. See also: <http://www.iza-structure.org>.

(5) Estermann, M.; McCusker, L. B.; Baerlocher, C.; Merrouche, A.; Kessler, H. *Nature* **1991**, *352*, 320–323.

(6) Férey, G. *C. R. Acad. Sci. Paris Ser. IIc* **1998**, *1*, 1 and references therein. Sassoie, C.; Loiseau, T.; Taulelle, F.; Férey, G. *Chem. Commun.* **2000**, 943.

(7) Wessels, T.; McCusker, L. B.; Baerlocher, C.; Reinert, P.; Patarin, J. *Microporous Mesoporous Mater.* **1998**, *23*, 67. Matijasic, A.; Paillaud, J.-L.; Patarin, J. *J. Mater. Chem.* **2000**, *10*, 1345.

(8) *Computer Modelling in Inorganic Crystallography*; Catlow, C. R. A., Ed.; Academic Press: London, 1997.

(9) van Beest, B. H. W.; Kramer, G. J.; van Santen, R. A. *Phys. Rev. Lett.* **1990**, *64*, 1955.

(10) Sanders, M. J.; Leslie, M.; Catlow, C. R. A. *J. Chem. Soc., Chem. Commun.* **1984**, 1271.

(11) Henson, N.; Cheetham, A. K.; Gale, J. D. *Chem. Mater.* **1994**, *6*, 1647.

(12) Gale, J. D.; Henson, N. J. *J. Chem. Soc., Faraday Trans.* **1994**, *90*, 3175.

(13) Henson, N. J.; Cheetham, A. K.; Gale, J. D. *Chem. Mater.* **1996**, *8*, 664.

the prediction of the calcined structure of an aluminophosphate, $\text{AlPO}_4\text{-14}$, starting from its experimentally determined templated form.¹⁴

In contrast, computational studies of GaPOs are very scarce. To our knowledge, no systematic attempt to rationalize their structures and physical properties using computational tools has been reported so far. This may arise from the complexity of these particular systems. Indeed, most gallium phosphates show complex chemical and structural features. Whereas zeolites are made exclusively of tetrahedrally coordinated metal atoms, there is a general trend for gallium atoms to occur in coordination numbers higher than those of aluminum, so that Ga can be found in 4-fold, 5-fold, or 6-fold coordinations. Another major feature of GaPOs is the diversity and complexity of their chemical compositions, arising from the frequent occurrence of charged template molecules or cations, hydroxy groups, bridging/terminal/encapsulated fluorine atoms, or structural water molecules, each of which may participate directly in the coordination sphere of the Ga metal atom. Also, GaPOs cover a wide range of Ga/P framework ratios, with the possibility of accommodating metal framework substitution, giving rise to the metallogallophosphate family. Another crucial issue is the understanding of the stabilities of GaPO inorganic frameworks, especially under severe conditions such as calcination treatments. In contrast with zeolites and AlPOs, where the organic species may often be removed, leaving behind an open-framework structure with potential adsorption or catalytic properties, the removal of template from GaPOs is a critical step that usually leads to the collapse of the structure. In any case, the production of the related stable open-framework compound cannot be rationally anticipated.

The scope of this work is the derivation of interatomic parameters for GaPOs, with the aim of initiating a systematic computational study of their structures. To date, there has been to our knowledge only one set of interatomic potentials for gallophosphate systems. Following the work of Kramer et al. on partial-charge rigid-ion models for silicates and aluminophosphates,⁹ Murashov used ab initio calculations on various clusters, including $[\text{Ga}(\text{OH})_4]^-$, $[\text{P}(\text{OH})_4]^+$, $(\text{HO})_3\text{GaOP}(\text{OH})_3$, and $\text{Ga}_2\text{P}_2\text{O}_4(\text{OH})_8$, to derive consistent potential parameters in order to study the molecular dynamics of α -quartz and low-cristobalite in their gallium phosphate forms.¹⁵

In the present work, we will derive a force field from a computational study of α -quartz-like GaPO_4 , using a formal charge shell model. The choice of developing this new force field in the limit of the ionic model has been motivated in order to allow compatibility with existing interatomic potentials for zeolites and related systems.^{10–14} The use of this type of potential in previous studies has shown that the Born model, when combined with polarizable oxygen usually through the use of a core–shell description, can successfully model a large variety of systems possessing metal atoms with oxidation states up to +5. Although formal charges do not have a better physical meaning than partial charges in such semi-ionic compounds, the use of a formal charge

rather than a partial charge based force field ensures better transferability to structures where Ga may have different local environments, ranging from tetrahedral to octahedral coordination, thus avoiding the problem in assigning different charges for Ga in distinct environments. An alternative solution would be to employ geometry-dependent charges, as determined according to an electronegativity equalization scheme. However, this would be more computationally demanding.

In the first section, we present the force field development based on the GaPO_4 –quartz structure. The GaPO_4 –quartz structure is the highest density gallium phosphate consisting of the strict alternation of $[\text{GaO}_4]^-$ and $[\text{PO}_4]^+$ tetrahedra, for which both experimentally determined structure¹⁶ and physical properties¹⁷ are available, yielding the required reference material needed for our force field development. In a second step, the transferability of the new force field to the study of gallosilicates and zeotype gallophosphates is considered.

Simulation Methods

Interatomic Potentials. The form of the interatomic potential chosen to describe the interaction between two ions i and j is a Buckingham potential combined with a Coulombic term to describe the electrostatic interactions

$$E_{ij} = A_{ij} \exp(-r_{ij}/\rho_{ij}) - Cr_{ij}^{-6} + q_i q_j / r_{ij} \quad (1)$$

where q_i and q_j refer to the charges of the ions and A_{ij} , ρ_{ij} , and C_{ij} are short-range potential parameters. The electrostatic energy is evaluated using an Ewald summation¹⁸ with the cutoff radii for the real and reciprocal space chosen so as to minimize the total number of terms to be calculated. The cutoff was chosen to give an accuracy of the order of 12 significant figures in the lattice energy. The short-range term was evaluated directly in real space with a cutoff radius of 12 Å.

Ionic polarizability for the oxygen atoms was incorporated using the simple mechanical model of Dick and Overhauser,¹⁹ in which an ion is represented by a core and a shell coupled by a harmonic spring

$$E_{\text{core-shell}} = 1/2k(r_{\text{core-shell}})^2 \quad (2)$$

where k is the core–shell spring constant. The shell model is primarily intended to simulate the dielectric properties of a material, especially those at high frequency, as well as the phonon dispersion.

The inclusion of three-body forces has also been considered in the form of a harmonic angle-bending potential

$$E_{ijk} = 1/2K(\theta_{ijk} - \theta_0) \quad (3)$$

where θ_0 is the equilibrium bond angle at the pivot atom j . All calculations have been performed using the program GULP.²⁰

Derivation of Potentials for GaPO_4 –Quartz. The development of the present force field comprised the empirical fitting of the potential parameters against GaPO_4 –quartz taken as a reference structure. The potential parameters are determined by a least-squares procedure which involves minimizing the weighted sum of squares of the differences between the experimental and calculated observables. Typi-

(16) Goiffon, A.; Bayle, G.; Astier, R.; Jumas, J. C.; Maurin, M.; Philippot, E. *Rev. Chim. Miner.* **1983**, *20*, 338.

(17) Palmier, D.; Goiffon, A.; Gohier, R.; Fischer, M.; Zarembovitch, A.; Philippot, E. *Ann. Chim., Sci. Mater.* **1997**, *22*, 627. Krempel, P.; Stadler, J.; Wallnöfer, W.; Ellmeyer, W.; Selic, R. *5th Eur. Freq. Time Forum, Besançon* **1991**, *4A-25*, 143.

(18) Ewald, P. P. *Ann. Phys.* **1921**, *64*, 253.

(19) Dick, B. G.; Overhauser, A. W. *Phys. Rev.* **1958**, *112*, 90.

(20) Gale, J. D. *J. Chem. Soc., Faraday Trans.* **1997**, *93*, 629.

(14) Girard, S.; Mellot-Draznieks, C.; Gale, J. D.; Férey, G. *Chem. Commun.* **2000**, 1161.

(15) Murashov, V. *Chem. Phys. Lett.* **1995**, *236*, 609.

cally, the observables include not only the crystal structure (cell parameters and atomic positions) but also the elastic and dielectric constants, which provide information about the curvature of the energy hypersurface. The procedure employed here is usually referred to as "relax fitting".²¹ Here a full optimization of the GaPO₄-quartz structure with a subsequent property calculation is performed at each point during the fitting procedure of force field parameters. Thus, the structural observables are the changes in the cell parameters and fractional coordinates rather than the stresses and atomic forces as used in conventional fitting. The experimental space group of the GaPO₄-quartz structure, *P*3₁21, was used as a constraint during the fitting procedure and subsequent minimization steps.

One major problem of empirical fitting is that of the weighting factors for observables. There is, in principle, an infinite number of optimum potential sets corresponding to distinct combinations of weighting factors. We have chosen to give an important weight to the structural parameters, i.e., atomic positions (10 000) and lattice parameters (1000), at the expense of other physical parameters such as elastic or dielectric constants (1) because these last properties are only meaningful if the structure is reasonably good.

Four successive steps in the development of the force field were performed. In the first fit, the potential parameters available for describing the P-O and O-O short-range interactions in aluminophosphates^{12,13} were held fixed and only the potential parameters for the Ga-O short-range interaction were fitted: i.e., $A_{\text{Ga-O}}$, $\rho_{\text{Ga-O}}$, and $C_{\text{Ga-O}}$. With such a fit it proved difficult to reproduce cell parameters and Ga-O bond lengths simultaneously with reasonable accuracy, leading to a systematic poor reproduction of Ga-O-P angles. In a second step, a harmonic Ga-O-P angle-bending potential was added to the energy expression in order to enforce an ideal second-neighbor environment for the gallium atoms. Simultaneous improvement of both cell size and bond lengths was obtained with a good representation of bond angles. However, the value for the Ga-O-P equilibrium angle in GaPO₄-quartz (134.6°) is not representative of the Ga-O-P angle distribution in other gallium phosphate structures, especially those having gallium in pentahedral or octahedral coordinations (Ga-O-P angles may range from 123.3 to 167.7° in ULM-4²² for example). Having this in mind, we replaced the Ga-O-P angle-bending potential term by a Ga-P repulsive potential. This third force field derivation yielded good reproduction of both cell parameters and bond lengths, therefore representing a reasonable compromise in terms of transferability. In a final fit, a further attempt to improve the force field consisted in the refinement of all parameters, including those of P-O and O-O pairs (A , ρ , C of both pairs) and the polarizability of the oxygen ion, (k_{O} , $q_{\text{O-shell}}$, $q_{\text{O-core}}$). Such a refinement led to little improvement, which fails to justify the resulting loss of compatibility implied with existing potentials for silicates and aluminophosphates. Consequently, the third set of potential parameters, which includes the Ga-P repulsive potential, was selected as the optimal force field and is given in Table 1.

Results and Discussion

Structure and Properties of GaPO₄-Quartz.

Both the energy-minimized GaPO₄-quartz structure obtained using our new force field and the experimental GaPO₄-quartz structure are shown in Table 2, together with the simulated and experimental elastic and dielectric constants. Figure 1 shows a superposition of both experimental and simulated structures. For further comparison, we also show in Table 2 the GaPO₄-quartz structure as optimized using the partial-charge rigid-ion potentials developed by Murashov.¹⁵ The corre-

Table 1. Potential Parameters Used for GaPO₄-Quartz within a Formal Charge Shell Model

	A/eV	$\rho/\text{\AA}$	$C/\text{eV \AA}^6$
Ga _{core} -O _{shell}	1950.797	0.2870	0.000
P _{core} -O _{shell}	877.340	0.3594	0.000
O _{shell} -O _{shell}	22764.000	0.1490	27.879
Ga _{core} -P _{core}			20.346
core-shell potential $k/\text{eV \AA}^{-2}$			
O	74.92		
atomic charge			
P	Ga	O _{core}	O _{shell}
+5	+3	+0.86902	-2.86902

sponding potentials are given in Table 3 for completeness.

The formal-charge shell model reproduces the experimental structure with reasonable accuracy, with the maximum deviation on the atomic positions being less than 0.06 Å with our force field as compared to 0.11 Å with that of Murashov. The new force field leads to an overestimation of the cell volume by 0.65%, while this is underestimated by 2.16% with the partial charge rigid-ion model. Despite the significant discrepancy regarding the reproduction of the cell parameter in the *c* direction, our force field shows a better local description of both the Ga and P cations environment in comparison with that obtained with Murashov's force field, especially for Ga-O and P-O interatomic distances.

Elastically, our model predicts GaPO₄-quartz to be too soft in all directions, while the rigid-ion model predicts it to be too hard. This is slightly counterintuitive, since the larger charges alone tend to make the formal charge model harder. Hence, this must largely be a consequence of the volume differences for the optimized structures. Regarding the reproduction of relative permittivities, while Murashov's potentials underestimate permittivities, the partial-charge shell model performs much better, especially for the reproduction of ϵ^0_{11} . This can be ascribed to the inclusion of polarizability, albeit in a simple fashion.

To the best of our knowledge there has been no experimental study of the phonon modes for GaPO₄-quartz; therefore, no comparison could be made. However, the calculation of the phonon modes of GaPO₄-quartz at the Γ point showed that both sets of potentials minimized the GaPO₄-quartz structure with no imaginary frequencies, thus demonstrating that the structure was phonon stable in the experimental space group.

As mentioned in section 2.2, further improvements of our force field were looked for with the fitting of additional force field parameters. However, considering that none of the structural or physical features of GaPO₄-quartz were significantly improved, and since this was at the cost of a loss of compatibility to existing potentials, these additional modifications of the force field were discounted.

Transferability of the Force Field to Gallosilicates. To address the validity of this force field and especially that of the new parameters associated with Ga atoms, we explored its application to the structural prediction of gallosilicates by performing energy minimizations of well-characterized structures. A range of 10 gallosilicates were chosen, where gallium atoms are

(21) Gale, J. D. *Philos. Mag. B* **1996**, *73*, 3.

(22) Cavellac, M.; Riou, D.; Férey, G. *Eur. J. Solid State Inorg. Chem.* **1994**, *31*, 583-594.

Table 2. Experimental/Calculated Structure and Properties for GaPO₄-Quartz, Using the Core-Shell Formal-Charge Model^a

	exptl	this work	Murashov ¹⁵		exptl	this work	Murashov ¹⁵
$a/\text{Å}$	4.899(1)	4.884	4.880	$\epsilon_{033}^0/10^9\text{N m}^{-2}$	6.7	5.4	2.0
$c/\text{Å}$	11.034(2)	11.171	11.000	Ga-O(1) (Å)	1.810	1.763	1.756
$V/\text{Å}^3$	229.339	230.829	224.384	Ga-O(2) (Å)	1.821	1.775	1.771
$C_{11}/10^9\text{N m}^{-2}$	6.6	5.45	7.30	P-O(1) (Å)	1.521	1.520	1.501
$C_{33}/10^9\text{N m}^{-2}$	10.2	8.70	13.22	P-O(2) (Å)	1.530	1.522	1.509
$C_{44}/10^9\text{N m}^{-2}$	3.78	2.48	4.05	$\langle\text{O-Ga-O}\rangle$ (deg)	110.26	110.66	110.66
$C_{66}/10^9\text{N m}^{-2}$	2.24	1.82	2.62	$\langle\text{O-P-O}\rangle$ (deg)	109.16	109.58	109.73
$\epsilon_{011}^0/10^9\text{N m}^{-2}$	6.3	6.3	2.0				

	x	y	z	x	y	z	x	y	z
Ga	0.4565(1)	0	1/3	0.4631	0	1/3	0.4510	0	1/3
P	0.4558(3)	0	5/6	0.4627	0	5/6	0.4461	0	5/6
O(1)	0.4069(7)	0.3169(7)	0.3928(2)	0.4143	0.3036	0.3964	0.4292	0.3187	0.3968
O(2)	0.4087(8)	0.2714(7)	0.8723(2)	0.4181	0.2693	0.8777	0.4096	0.2686	0.8804

^a This work. The energy-minimized GaPO₄-quartz structure obtained with the rigid-ion partial-charge model from ref 15 is shown for comparison.

not only in tetrahedral coordination but also in octahedral coordination. In this selection, both open-framework zeotype structures and dense structures were considered, for which crystallographic data were available from either single-crystal or powder diffraction refinements.

Four zeotype gallosilicates were selected with various Si/Ga ratios (1.4–3.5) and with charge-compensating extraframework cations such as Na⁺ and K⁺: Na₄Si₆Ga₄O₂₀ (NAT),²³ K₉Si₂₇Ga₉O₇₂ (LTL),²⁴ Na₄Si₁₄Ga₄O₃₆ (MAZ),²⁵ and Na₅Si₇Ga₅O₂₄ (SOD),²⁶ the last two being in hydrated forms. Gallium atoms are systematically in tetrahedral coordination, and the framework consists of the arrangement of corner-sharing GaO₄ and SiO₄ tetrahedra. However, in all these crystal structures, Ga and Si atoms were not refined independently, with a consequently disordered distribution of Si and Ga atoms over their crystallographic sites. In addition, occurrence of partial occupancies for cationic sites is reported for some structures.

Six dense minerals were also considered: KGaSi₃O₈,²⁷ SrGa₂Si₂O₈,²⁸ NaGaSi₂O₆,²⁹ BaGa₂Si₂O₈,³⁰ Na_{0.7}K_{0.3}GaSiO₄,³¹ and Ca₃Ga₂Si₃O₁₂.³² Among them, tetrahedral and octahedral coordinations are found for gallium atoms. The Si/Ga ratio ranges from 1 to 3, with various extraframework cations (Na⁺, K⁺, Ba²⁺, Ca²⁺, Sr²⁺). Again, some structures show a disordered distribution of framework (Ga, Si) atoms over equivalent T-sites and partial occupancies for cationic sites.

A summary of the chemical and structural features of the selected gallosilicates is given in Table 4. All these structures provide a good experimental basis for validating our force field, owing to the considerable differ-

ences between their chemical and structural features: the Si/Ga ratio (1–3.5), the density (2.06–4.10 g/cm³), the charge-compensating cation, and also the gallium coordination number.

The crystallographic data for these structures were used directly as starting models for energy minimization, except for the sodalite- and natrolite-type structures, where adsorbed water molecules were removed prior to the simulations. The treatment of disorder and partial occupancies was handled through the use of mean field theory (virtual crystal approximation). In practice, all interactions just become weighted by the product of the site occupancies of the atoms involved. In addition, when two atoms share a site with partial occupancy, they are constrained to move as a single ion during the optimization and do not interact with each other. At first, structures with disorder may not seem ideal for testing specific force field parameters. However, such disordered structures are often averaged in a similar fashion through crystal refinements; thus, we believe that comparing crystallographic data and simulated structures is a reasonable approach.

All the gallosilicates were subjected to constant-pressure energy minimization using the Ga–O short-range parameters developed above and the Si–O and cation–O parameters developed by Catlow et al. for the simulation of silicates and aluminosilicates.^{10,33} Regarding the extraframework cations, the force field parameters were taken from refs 33 and 34, where nonzeolite potentials were relax-fitted to structures and any available properties for the relevant binary oxides (Na₂O, K₂O, BaO, CaO and SrO). The phonon spectra at the Γ point for all the structures were calculated, and they were all found to be phonon stable in their space group.

Table 5 shows a comparison of our calculated lattice parameters and space groups with experimental data. The lattice parameters are reproduced within 5% of the experimental values, with a trend for an overestimation. The differences between the experimental and simulated structures may arise due to various reasons, besides the presence of disordered sites. (i) The Si–O and O–O potential parameters were derived from SiO₂–quartz, and their robustness was validated on a large

(23) Xie, D.; Newsam, J. M.; Yang, J.; Yelon, W. B. *Mater. Res. Soc. Symp. Proc.* **1988**, *111*, 147.

(24) Newsam, J. M. *Mater. Res. Bull.* **1986**, *21*, 661.

(25) Newsam, J. M.; Jarman, R. H.; Jacobson, A. J. *Mater. Res. Bull.* **1985**, *20*, 125.

(26) Newsam, J. M.; Jorgensen, J. D. *Zeolites* **1987**, *7*, 569.

(27) Kimata, M.; Saito, S.; Shimizu, M. *Eur. J. Mineral.* **1995**, *7*, 287.

(28) Phillips, M. W.; Kroll, H.; Pentinghaus, H. *Am. Mineral.* **1975**, *60*, 659.

(29) Ohashi, H.; Osawa, T.; Sato, A. *Acta Crystallogr.* **1995**, *C51*, 2476.

(30) Kroll, H.; Phillips, M. W.; Pentinghaus, H. *Acta Crystallogr.* **1978**, *B34*, 359.

(31) Barbier, J.; Liu, B.; Weber, J. *Eur. J. Mineral.* **1993**, *5*, 297.

(32) Novak, G. A.; Gibbs, G. V. *Am. Mineral.* **1971**, *56*, 791.

(33) Jackson, R. A.; Catlow, C. R. A. *Mol. Simul.* **1988**, *1*, 207.

(34) Gale, J. D. Unpublished results.

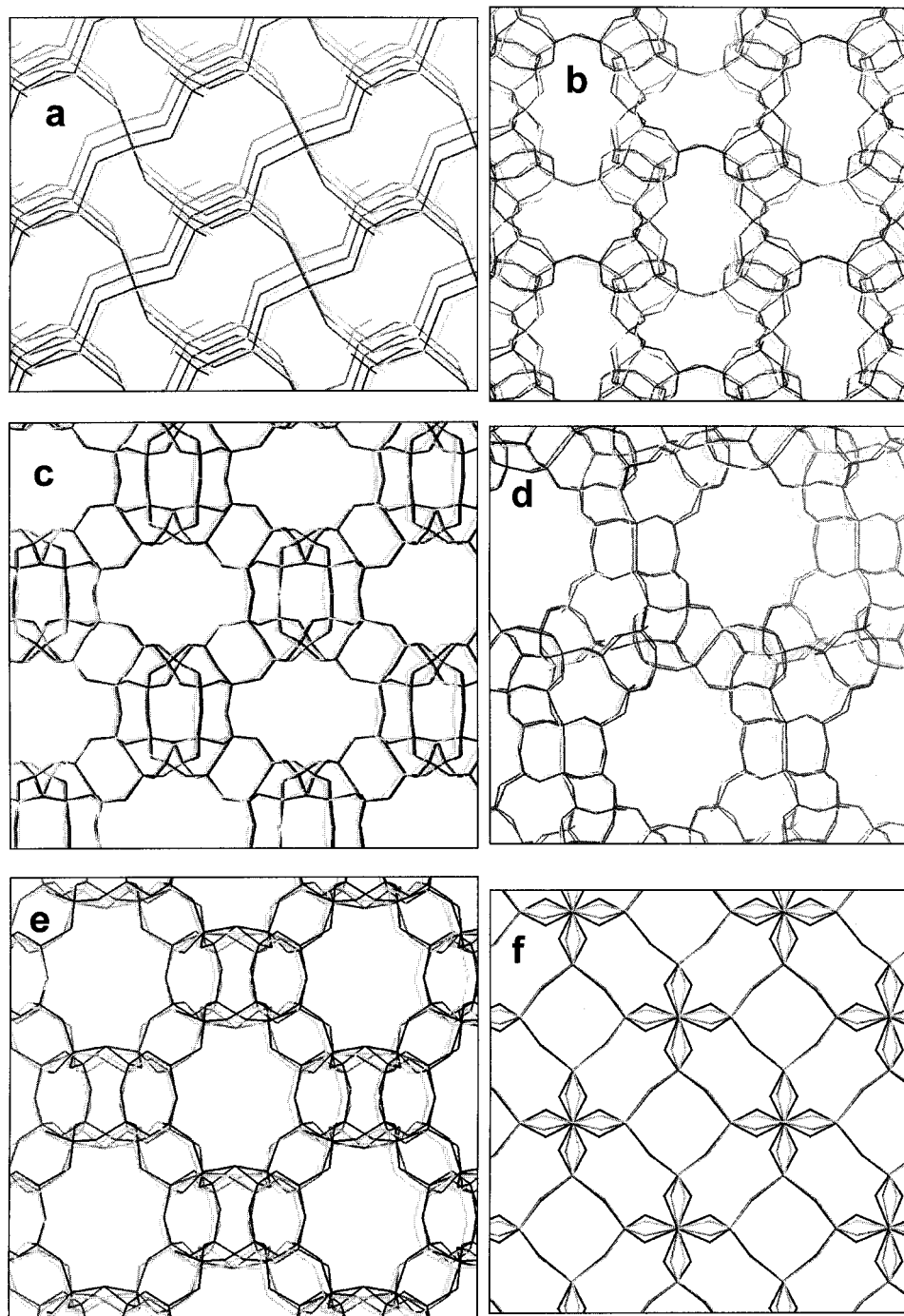


Figure 1. Comparison between experimental (black) and simulated (gray) frameworks for various gallophosphates: (a) GaPO_4 -quartz; (b) GaPO_4 -CGF; (c) GaPO_4 -CGS; (d) GaPO_4 -SBT; (e) GaPO_4 -LAU; (f) GaPO_4 -SOD.

Table 3. Potential Parameters from Ref 15 by Murashov, within a Partial Charge Rigid-Ion Model

	A/eV	$\rho/\text{\AA}$	$C/\text{eV \AA}^6$
$\text{Ga}_{\text{core}}-\text{O}_{\text{core}}$	20955.5346	0.21576	222.2168
$\text{P}_{\text{core}}-\text{O}_{\text{core}}$	9034.2080	0.19264	19.8793
$\text{O}_{\text{core}}-\text{O}_{\text{core}}$	1388.7730	0.36232	175.0000
atomic charge			
P	Ga	O	
+3.4	+1.4	-1.2	

number of structures. In contrast, the potential parameters used for O-cation interactions have been tested far less often. (ii) The presence of water molecules is

usually known to have a significant impact on cell parameters, through the formation of weak hydrogen bonds with the framework oxygens for example.

With these factors in mind, the agreement between experimental and simulated gallosilicates cannot be as impressive as was found in the case of silicates and aluminophosphates. For example, the Sanders potential reproduced a wide variety of silicates with an error on cell parameters lower than 2% and the Gale and Henson potential reproduced many aluminophosphates with an error on cell parameters lower than 3.7%. Nevertheless, the accuracy obtained with our potential shows it is of sufficient quality to yield good structural predictions of various dense and microporous gallosilicates, especially

Table 4. Chemical and Structural Features of Various Existing Gallosilicates

formula	struct type	Ga coord	Si/Ga ratio	cation	disorder partial occ	density/(g/cm ³)
<i>n</i> H ₂ O, Na ₄ Si ₆ Ga ₄ O ₂₀	natrolite	IV	1.5	Na ⁺	Ga/Si Na ⁺	2.47
K ₉ Si ₂₇ Ga ₉ O ₇₂	LTL	IV	3	K ⁺	Ga/Si K ⁺	2.14
Na ₄ Si ₁₄ Ga ₄ O ₃₆	mazzite	IV	3.5	Na ⁺	Ga/Si Na ⁺	2.06
<i>n</i> H ₂ O, Na ₅ Si ₇ Ga ₅ O ₂₄	sodalite	IV	1.4	Na ⁺	Ga/Si Na ⁺	2.66
KGaSi ₃ O ₈	feldspar	IV	3	K ⁺	Ga/Si	2.89
SrGa ₂ Si ₂ O ₈	feldspar	IV	1	Sr ²⁺	none	3.55
NaGaSi ₂ O ₆	pyroxene	VI	2	Na ⁺	none	3.89
BaGa ₂ Si ₂ O ₈	feldspar	IV	1	Ba ²⁺	none	4.02
Na _{0.7} K _{0.3} Ga-SiO ₄	kalsilite	IV	1	Na ⁺	Ga/Si	3.31
Ca ₃ Ga ₂ Si ₃ O ₁₂	garnet	VI	1.5	K ⁺ Ca ²⁺	Na/K none	4.10

Table 5. Comparison of Experimental (Roman Type) and Calculated (Italic Type) Cell Parameters for Gallosilicates

structure	space group	<i>a</i> (Å)	<i>b</i> (Å)	<i>c</i> (Å)	β (deg)	ref
natrolite	<i>Fdd</i> 2	18.423 <i>17.834</i>	18.826 <i>18.821</i>	6.652 <i>6.529</i>		23
LTL	<i>P6/mmm</i>	18.580 <i>18.646</i>		7.489 <i>7.717</i>		24
mazzite	<i>P6₃/mmc</i>	18.043 <i>18.274</i>		7.662 <i>7.737</i>		25
sodalite	<i>P4₃n</i>	8.848 <i>9.280</i>				26
KGaSi ₃ O ₈	<i>C2/m</i>	8.660 <i>9.185</i>	13.102 <i>13.031</i>	7.229 <i>7.236</i>	116.06 <i>115.06</i>	27
SrGa ₂ Si ₂ O ₈	<i>P2₁/a</i>	9.001 <i>9.236</i>	9.484 <i>9.479</i>	8.399 <i>8.582</i>	90.68 <i>90.76</i>	28
NaGaSi ₂ O ₆	<i>C2/c</i>	9.557 <i>9.553</i>	8.702 <i>8.478</i>	5.270 <i>5.238</i>	107.64 <i>104.54</i>	29
BaGa ₂ Si ₂ O ₈	<i>C2/c</i>	8.726 <i>8.908</i>	13.212 <i>12.963</i>	14.600 <i>14.549</i>	115.06 <i>113.62</i>	30
Na _{0.7} K _{0.3} Ga-SiO ₄	<i>P6₃</i>	8.817 <i>9.081</i>		8.387 <i>8.579</i>		31
Ca ₃ Ga ₂ Si ₃ O ₁₂	<i>Ia3d</i>	12.020 <i>11.948</i>				32

with the reproduction of structures including gallium atoms in octahedral coordination.

Transferability of our Model to Gallophosphates. We derived gallophosphate models from the following metalgallophosphates (MeGaPOs), since the only structural data available for such systems were for their MeGaPO derivatives: (C₇NH₁₄)CoGa₃P₄O₁₆-CGS,³⁵ (C₃N₂H₅)₈Co₈Ga₁₆P₂₄O₉₆-LAU,³⁶ (CN₃H₆)ZnGaP₂O₈-GIS,³⁷ (C₆N₂H₁₄)₂Co₄Ga₅P₉O₃₆-CGF,³⁸ (C₉N₂H₂₂)Co₂Ga₂P₄O₁₆-SBS,³⁹ (C₁₀O₃N₂H₂₄)Zn₂Ga₂P₄O₁₆-SBT,³⁹ and (NC₄H₁₂)ZnGa₂P₃O₁₂-SOD.⁴⁰ All these structures have zeotype architectures made of corner-sharing tetrahedra, with a tetrahedral environment for all metal atoms, including Co and Zn atoms. The presence of in-framework M²⁺ (Co²⁺, Zn²⁺) metal atoms generates an

Table 6. Comparison of Experimental (Roman Type) and Calculated (Italic Type) Cell Parameters for Gallophosphates

	space group	vol (Å ³)	<i>a</i> (Å)	<i>b</i> (Å)	<i>c</i> (Å)	β (deg)	ref
GaPO ₄ -CGS	<i>P2₁/c</i>	2045.67 <i>2003.66</i>	14.365 <i>14.377</i>	16.305 <i>16.070</i>	8.734 <i>8.672</i>	90.24 <i>90.02</i>	35
GaPO ₄ -LAU	<i>C2/c</i>	2727.37 <i>2780.75</i>	14.981 <i>14.572</i>	12.953 <i>13.126</i>	15.144 <i>15.511</i>	111.86 <i>110.41</i>	36
GaPO ₄ -GIS	<i>I2/a</i>	968.82 <i>995.27</i>	10.041 <i>9.796</i>	9.220 <i>10.373</i>	10.469 <i>9.796</i>	91.60 <i>91.06</i>	37
GaPO ₄ -CGF	<i>I2/a</i>	4146.29 <i>4045.71</i>	15.002 <i>14.800</i>	17.688 <i>17.327</i>	15.751 <i>15.850</i>	97.24 <i>95.54</i>	38
GaPO ₄ -SBS	<i>P3₁c</i>	7488.71 <i>7417.59</i>	17.836 <i>17.464</i>			27.182 <i>28.082</i>	39
GaPO ₄ -SBT	<i>R3</i>	11875.99 <i>11106.11</i>	18.080 <i>17.466</i>			41.951 <i>42.039</i>	39
GaPO ₄ -SOD	<i>P4₃n</i>	711.93 <i>715.77</i>	8.9292 <i>8.945</i>				40

Table 7. Comparison of Experimental (Roman Type) and Calculated (Italic Type) Average Bond Lengths and Angles for Model Gallophosphates

	\langle Ga-O \rangle (Å)	\langle P-O \rangle (Å)	\langle O-Ga-O \rangle (deg)	\langle O-P-O \rangle (deg)
GaPO ₄ -CGS	1.839 <i>1.761</i>	1.524 <i>1.519</i>	109.42 <i>109.47</i>	109.46 <i>109.47</i>
GaPO ₄ -LAU	1.855 <i>1.759</i>	1.523 <i>1.518</i>	109.47 <i>109.45</i>	109.47 <i>109.47</i>
GaPO ₄ -GIS	1.868 <i>1.751</i>	1.527 <i>1.515</i>	109.44 <i>109.46</i>	109.45 <i>109.47</i>
GaPO ₄ -CGF	1.868 <i>1.762</i>	1.517 <i>1.519</i>	109.46 <i>109.44</i>	109.48 <i>109.47</i>
GaPO ₄ -SBS	1.876 <i>1.758</i>	1.519 <i>1.518</i>	108.41 <i>109.47</i>	109.46 <i>109.47</i>
GaPO ₄ -SBT	1.897 <i>1.759</i>	1.548 <i>1.518</i>	109.36 <i>109.46</i>	109.45 <i>109.47</i>
GaPO ₄ -SOD	1.8552 <i>1.7456</i>	1.5276 <i>1.5134</i>	109.48 <i>109.47</i>	109.48 <i>109.48</i>

anionic framework that is compensated by the protonated template molecules.

No attempt was made to take the template molecules into account in our calculations, since our aim is to address the applicability of our new force field to the simulation of the structure of gallophosphate frameworks in the absence of template molecules. To build models that are appropriate for energy-minimization calculations, we derived the gallophosphates from their as-synthesized metalgallophosphate analogues as follows.

The template molecules were systematically removed, while framework Co²⁺/Zn²⁺ metal atoms were replaced by Ga³⁺ atoms in each structure, leaving behind a series of neutral open-framework structures with identical chemical compositions, namely GaPO₄. We checked that no change of symmetry was produced upon the Co,Zn/Ga substitution. These gallophosphate models were then submitted to constant-pressure energy minimizations.

In Table 6, we show a comparison of our calculated lattice parameters and space groups with experimental data. Except for the gismondine-like structure, the lattice parameters are reproduced with good accuracy within 3.4% of the experimental values. Table 7 shows a comparison of average interatomic distances (\langle Ga-O \rangle , \langle P-O \rangle) and angles (\langle O-Ga-O \rangle , \langle O-P-O \rangle) between experimental and simulated structures. While \langle P-O \rangle distances are reproduced with very good accuracy, discrepancies between experimental and simulated

(35) Cowley, A. R.; Chippindale, A. M. *Microporous Mesoporous Mater.* **1999**, *28*, 163.

(36) Bond, A. D.; Chippindale, A. M.; Cowley, A. R.; Readman, J. E.; Powell, A. V. *Zeolites* **1997**, *19*, 326.

(37) Chippindale, A. M.; Cowley, A. R.; Peacock, K. J. *Microporous Mesoporous Mater.* **1998**, *24*, 133.

(38) Chippindale, A. M.; Cowley, A. R. *Zeolites* **1997**, *18*, 176.

(39) Bu, X.; Feng, P.; Stucky, G. D. *Science* **1997**, *278*, 2080.

(40) Bu, X.; Gier, T. E.; Feng, P.; Stucky, G. D. *Microporous Mesoporous Mater.* **1998**, *20*, 371.

$\langle\text{Ga-O}\rangle$ distances may be assigned to modifications of M–O bond lengths and O–M–O angles upon the Co,Zn/Ga substitution in the model structures. Also, the present work explores gallophosphates in their template-free form, while the experimental crystal structure data refers to templated structures, which may induce local distortions in the framework that are not taken into account in our simulations. The superposition of the experimental and simulated frameworks for five structures are presented in Figure 1.

In the case of the gismondine-type structure, the flexibility of the framework is well-known in aluminosilicate and aluminophosphate analogues. For example, the use of guanidinium chloride or pyrrolidine during the synthesis of zinc gallium phosphates leads to two materials with the gismondine-type framework topology, but with different cell parameters, space groups, and cage shapes.³⁷ The structural data for these two compounds are compared in Table 8. The flexibility of the gismondine-type framework depends on the chemical composition and may account for the large differences we observe between the experimental structure and its GaPO_4 simulated form.

Hence our potential reproduces model gallophosphate structures with a reasonable accuracy. Once again, the experimental space groups gave no imaginary frequencies in the phonon spectrum, and so the seven structures are stable in their experimentally determined space groups.

Table 8. Comparison of the Structures of Two ZnGaPO_4 Materials with the Same Gismondine Framework Topology

	$(\text{CN}_3\text{H}_6)[\text{ZnGaP}_2\text{O}_8]$	$(\text{C}_4\text{NH}_{10})[\text{ZnGaP}_2\text{O}_8]$
cryst syst	monoclinic	orthorhombic
space group	<i>I2/a</i>	<i>Fddd</i>
vol (\AA^3)	969.20	2181.29
<i>a</i> (\AA)	10.041	9.993
<i>b</i> (\AA)	9.220	14.525
<i>c</i> (\AA)	10.469	15.028
β (deg)	91.6	90.0

Conclusions

Here we have developed a new set of potentials for the study of gallophosphates. Our model for GaPO_4 –quartz is compatible with existing potentials available for the study of zeolites. These interatomic potentials, combined with the one developed by Gale and Henson,¹² allows the study of many dense or microporous materials containing Si, Al, Ga, or P atoms at the center of the polyhedra that compose the framework. In addition to being applicable to gallophosphates, this force field also transfers well to gallosilicates. In a future publication, we intend to use this new force field to explore the framework stabilities and crystal structures of various families of open-framework gallophosphates.

CM001233S